



Effect of Damage on Natural Vibration Characteristics of Large Semi-cushion Spiral Case Structure

Bo Xu¹ · Hui Xia²

Received: 10 May 2017 / Accepted: 4 April 2018 / Published online: 10 April 2018
© King Fahd University of Petroleum & Minerals 2018

Abstract

A spiral case structure presents various natural vibration characteristics with damage in different degrees in peripheral concrete. The natural vibration characteristics and resonance safety of a large semi-cushion spiral case structure with damage in varying degrees in peripheral concrete are compared and analyzed. For this purpose, a finite element analysis method of vibration characteristics, a four-parameter damage constitutive model of concrete, and spiral case structure of the Ahai Hydropower Station are utilized. Results show that each mode of natural frequency of the spiral case structure declines after the damage in concrete. The extent of the reduction in natural frequency is large when the damage is serious. The mode shapes of the spiral structure are all complex and twisted before and after the damage in concrete. Afterward, however, amplitude increases. After considering the damage, a new possible source of resonance cannot be identified. Resonance checking shows that the damage in concrete cannot seriously harm the Ahai spiral case structure. Therefore, this study provides new reference and support for the production design and safe operation of large semi-cushion spiral case structure.

Keywords Large semi-cushion spiral case structure · Natural vibration characteristic · Concrete damage · Resonance checking · Four-parameter damage model · Finite element method

1 Introduction

The rapid development of large hydropower stations has facilitated the continued establishment of hydropower stations with large heads and capacity. The scale and unit capacity of these stations increases with the size of their spiral case structure. The height of the bearing water head of spiral case structure increases, and the parameters of its design in the current code are no longer applicable. Hence, studies on large and giant spiral case structures are crucial [1]. Vibration problems exist in various houses in hydropower stations. These issues seriously affect normal operations, cause detrimental effects on hydropower stations, and concern operators. Vibration and stability problems become prominent with the increase in unit capacity.

Studies conducted in various countries show that damage exerts a certain effect on the natural vibration characteristics of structures. Ditommaso et al. [2] studied the fundamental period of reinforced concrete buildings and its variation in four damage levels. Hamad et al. [3] studied the degradation of vibration characteristics of reinforced concrete beams owing to flexural damage through experiments and numerical simulation with an improved crack model. Wang and Ren [4] investigated the relationship between local damage and structural dynamic behavior of a three-dimensional steel frame structure through an experiment. Sevim et al. [5] evaluated the effects of crack on the dynamic characteristics of a prototype arch dam by using ambient vibration tests. Altunişik et al. [6–8] investigated changes in dynamic properties of damaged and strengthened arch dam models with and without reservoir water. Altunişik et al. [9] also investigated the dynamic characteristics of undamaged and damaged beams through calculation and measurements. Altunişik [10] studied the effect of damage and time on the dynamic characteristics of a box girder bridge model using ambient vibration tests. Various studies have also been conducted on the effect of damage on the natural vibration characteristics of spiral case structure. Zhang et al. [11] and

✉ Bo Xu
xubo@yzu.edu.cn

¹ School of Hydraulic, Energy and Power Engineering, Yangzhou University, Yangzhou 225127, China

² Jiangsu Surveying and Design Institute of Water Resources Co., Ltd., Yangzhou 225127, China

Tian et al. [12] studied the influence of damage caused by fluctuating load on the natural vibration characteristics and examined the effect of concrete cracks on the dynamic characteristics of the directly embedded spiral case structure in the Three Gorges Hydropower Station, respectively. These studies indicate that the spiral case structure is an important flow component of a hydropower house. Local damage in this structure can exert a certain effect on its natural vibration characteristics and compromise its vibration safety. Therefore, examining the influence of local structural damage on the natural vibration characteristics and vibration safety of the large spiral case structure is crucial.

The application of the large cushion spiral case in hydropower stations with high head and large capacity is extensive. Thus, research on the large cushion spiral case is crucial to meet the actual needs of the projects. A semi-cushion spiral case is a special type, in which cushion is laid only in a certain area on the upper external surface of certain parts, such as the straight pipe section of the steel spiral case. In this study, the influence of damage in varying degrees on the natural vibration characteristics of large semi-cushion spiral case structure is investigated.

2 Four-Parameter Damage Model of Concrete

2.1 Four-Parameter Failure Criterion for Concrete

We study the influence of different degrees of damage in concrete on the natural vibration characteristics of large semi-cushion spiral case structure. To achieve this aim, a four-parameter failure criterion is used to simulate the damage in concrete structure, which is established on the strain space as follows [13]:

$$F(I'_1, J'_2, \varepsilon_1) = a \frac{J'_2}{\varepsilon_p} + b\sqrt{J'_2} + c\varepsilon_1 + dI'_1 - \varepsilon_p = 0, \quad (1)$$

where $I'_1 = \varepsilon_{ii}$ ($i = 1, 2, 3$) is the first invariant of strain tensor. $J'_2 = e_{ij}e_{ij}/2$ ($i, j = 1, 2, 3$) is the second invariant of strain deviation. $\varepsilon_1 = \frac{2}{\sqrt{3}}\sqrt{J'_2} \sin(\theta + \frac{2}{3}\pi) + \frac{1}{3}I'_1$ is the maximum principal strain, and $\theta = \frac{1}{3}\arcsin(-\frac{3\sqrt{3}J'_3}{2\sqrt{J'_2^3}})$, $|\theta| \leq 60^\circ$. $J'_3 = e_{ij}e_{jk}e_{ki}/3$ ($i, j, k = 1, 2, 3$) is the third invariant of strain deviation.

The tensile strength of concrete is significantly lower than its compressive strength. The value of ε_p is $\varepsilon_p = C_t f_c / E = f_t / E$, where f_t is the tensile strength of the material. f_c is the compressive strength of the material. C_t is the ratio of tensile to compressive strength. E is the elastic modulus of

the material. Parameters a , b , c , and d can be determined using the four groups of strength test data.

2.2 Four-Parameter Equivalent Strain for Concrete

On the basis of the principle, we assume that the four-parameter failure criterion is applicable to the strain softening stage and that the parameters are the same. We use equivalent strain ε^* to replace ε_p , such that the four-parameter equivalent strain of isotropic damage model is obtained as follows:

$$\varepsilon^* = a \frac{J'_2}{\varepsilon^*} + b\sqrt{J'_2} + c\varepsilon_1 + dI'_1. \quad (2)$$

The definitions of variables in Formula (2) are provided in Formula (1).

Formula (2) is a quadratic formula on ε^* . By solving the quadratic formula, we can calculate equivalent strain ε^* under various stress states as follows:

$$\varepsilon^* = \frac{(b\sqrt{J'_2} + c\varepsilon_1 + dI'_1) \pm \sqrt{(b\sqrt{J'_2} + c\varepsilon_1 + dI'_1)^2 + 4aJ'_2}}{2}. \quad (3)$$

The equivalent strain cannot be negative. Thus, the positive solution of Formula (3) can only be regarded as

$$\varepsilon^* = \frac{(b\sqrt{J'_2} + c\varepsilon_1 + dI'_1) + \sqrt{(b\sqrt{J'_2} + c\varepsilon_1 + dI'_1)^2 + 4aJ'_2}}{2}. \quad (4)$$

2.3 Solution of Damage Variables

According to the equivalent strain principle of concrete damage theory, the constitutive relation of concrete is as follows:

$$\sigma = \sigma(\varepsilon, \varepsilon_p, D) = \varepsilon E_0(1 - D), \quad (5)$$

where ε_p is the strain corresponding to peak stress. D is the damage variable, assuming that material initial damage D_0 is zero. E_0 is the elastic modulus when the material exhibits no damage.

In the case of uniaxial stress, the tensile stress–strain curve can be expressed as follows:

Rising curve ($\varepsilon/\varepsilon_p \leq 1$):

$$\frac{\sigma}{\sigma_p} = \frac{\varepsilon/\varepsilon_p}{0.8(1 - \varepsilon/\varepsilon_p)^{1.8} + \varepsilon/\varepsilon_p}. \quad (6)$$

Decline curve ($\varepsilon/\varepsilon_p > 1$):

$$\frac{\sigma}{\sigma_p} = \frac{\varepsilon/\varepsilon_p}{1.2(1 - \varepsilon/\varepsilon_p)^2 + \varepsilon/\varepsilon_p}, \tag{7}$$

where σ_p is the peak stress of uniaxial tension and ε_p is the strain corresponding to peak stress.

On the basis of the stress–strain curve in Formulas (6) and (7) and in accordance with Formula (5), the damage variable can be obtained as follows:

$$D = 1 - \frac{\sigma}{E_0\varepsilon}. \tag{8}$$

For the multi-axial stress condition, ε in Formula (8) can be transformed into equivalent strain ε^* . In addition, corresponding damage variable can be obtained.

3 Analysis of Influence of Damage on Natural Vibration Characteristics

The natural vibration characteristics of structure include natural frequency and mode shape. The finite element dynamic equilibrium formula is as follows:

$$[K] \{\delta\} + [C] \{\dot{\delta}\} + ([M] + [M_p]) \{\ddot{\delta}\} = [R_0], \tag{9}$$

where C and K are the damping and stiffness matrices of the structure, respectively. δ , $\dot{\delta}$, and $\ddot{\delta}$ are the nodal displacement, velocity, and acceleration vectors, respectively. R_0 is the external load vector. M is the mass matrix of structure and $[M_p]$ is the additional mass matrix.

The stiffness of spiral case structure is relatively large, and the spiral case is a type of high-frequency structure with high natural frequency. The influence of water mass on the natural vibration characteristics of spiral case structure is limited. Hence, the additional mass method can be used to approximately consider the influence of water mass on the natural vibration characteristics of spiral case structure. In addition, the additional mass method does not require the establishment of the finite element model and meshing for water body and possesses high calculation efficiency. In this study, the Westergaard additional mass method is applied to approximately simulate the influence of water mass. In addition, the calculation formula of the additional mass matrix $[M_p]$ in this method is as follows:

$$M_p = \frac{7}{8} \rho A \sqrt{hy}. \tag{10}$$

In practical engineering, the influence of damping on the natural frequencies and mode shapes of structure is minimal.

Damping force can be disregarded, and the free vibration formula without damping is as follows:

$$([K] - \omega^2 [\bar{M}]) \{\delta_0\} = 0. \tag{11}$$

In the formula, $[\bar{M}] = [M] + [M_p]$.

When calculating the natural vibration characteristics of structure without damage, the stiffness matrix K in Formula (11) is the original stiffness matrix K_0 of the structure. When calculating the natural vibration characteristics of structure with damage, the stiffness matrix K in Formula (11) is the stiffness matrix K_D of the damaged structure.

In the seismic calculation of hydraulic structures, only a few of the lowest frequencies are usually computed. In this case, the direct filtering frequency method based on the inverse power method is simple and effective. We employ the direct filtering frequency method to calculate the natural frequencies and mode shapes of structure.

The influence of damage on the vibration characteristics of large semi-cushion spiral case structure is analyzed as follows:

- (1) A 3D finite element model of spiral case structure is established.
- (2) The damage in the spiral case structure is analyzed under different overload schemes based on the four-parameter damage model of concrete.
- (3) The direct filtering frequency method is used to calculate the natural frequencies and mode shapes of spiral case structure in accordance with damage under different overload schemes. The influence of damage on natural vibration characteristics is investigated.
- (4) Further analysis on the influence of damage on the natural vibration characteristics is conducted by analyzing and comparing the resonance safety of natural and forced vibration frequencies under various damage conditions.

4 Engineering Example

4.1 Basic Data

(1) Model scope

The intake section diameter of the Ahai Hydropower Station is 9.85 m. The thickness of the steel liner is 21–56 mm. A unit is considered the object of calculation and analysis. The upstream boundary is located at the divided joint department of the plant and dam, while the downstream boundary is found at the external surface of the downstream wall of the main building. The distance from upstream to downstream is 34.10 m. Both sides are divided by the permanent joints of the unit and comprise a total distance of 34.00 m from left

to right. A basic elevation of 1,423.135 m of the upper stator of the hydraulic turbine is the upper boundary. A bottom elevation of 1,400.00 m of the straight cone section of the draft tube is the boundary at the bottom. This area comprises a total of 23.135 m. The cushion is laid on the straight pipe section of the intake and part of the bend pipe section, and its thickness is 30 mm.

(2) Coordinate system

The calculation model is based on the Cartesian coordinates. The X axis lies in the horizontal direction, and the left direction (facing downstream) or along the longitudinal axis of the building is positive. The Y axis also lies in the horizontal direction, and the direction pointing upstream is positive. The Z axis lies in the vertical direction, and the upward direction is positive. The coordinate origin is found at the intersection of the installation elevation for the hydraulic turbine and unit axis.

(3) Model component and element type

The model is divided into six parts, namely stay ring, guide vanes, steel liner, straight cone section of the draft tube, concrete, and cushion. We use four-node plate bending elements to simulate the steel liner, stay ring, guide vanes, and straight cone section of the draft tube. Eight-node hexahedron elements are used to simulate the surrounding concrete and cushion. The model comprises 50,274 elements and 52,106 nodes. The steel liner, stay ring, guide vanes, straight cone section of draft tube, surrounding concrete, and cushion are divided into 3,272, 480, 820, 600, 44,262, and 840 elements, respectively. The schematic of the model is shown in Fig. 1.

(4) Material properties

Tensile strength f_t of concrete is 1.75 MPa. Compressive strength f_c of concrete is 17 MPa. The ratio of tensile to compressive strength, C_t , is 0.10294. Parameters a , b , c , and d of the failure criterion are 0.0132, 0.1239, 0.7469, and 0.2456, respectively. The remaining material parameters are shown in Table 1.

(5) Boundary condition and contact properties

The bottom of the calculation model is considered multi-constrained, whereas the outer boundaries of the structure are considered free surfaces. The effect of friction contact of concrete, steel liner, and cushion is analyzed using the gap element method. In the analysis, the friction coefficient is 0.25, while cohesion is 10^3 kPa.

(6) Loads

The loads related to the spiral case of the hydraulic turbine under normal operation of the hydropower station are considered as follows: (1) dead weight of each part of the structure, (2) uniform live load of 40 kN/m^2 on the hydraulic turbine, (3) load of each stator at 344 KN (the stator consists of 18 foundation plates), (4) load of each low bracket at 2,916 KN (the low bracket consists of 12 foundation plates), (5) water pressure in the cavity of the spiral case of 105.6 m water head pressure, (6) hydrostatic pressure of the annular

plate on the stay ring from the top cover of the hydraulic turbine is approximately considered the hydrostatic pressure at the location of the unit installation elevation, and (7) water pressure of the tail pipe is the pressure produced by normal tail water level.

4.2 Calculation and Analysis

Six schemes are selected in analyzing the influence of damage on natural vibration characteristics. These schemes are as follows: Scheme 1 in which the damage in concrete is not considered; scheme 2 in which the damage in concrete under the design load is considered; and schemes 3, 4, 5, and 6 in which the damage in concrete when the structure bears overload at 1.5, 2, 2.5, and 3 times that of the water load are considered, respectively.

4.2.1 Analysis of Concrete Damage

Figures 2, 3, 4, 5, and 6 show the damage conditions of concrete corresponding to schemes 2–6, respectively. From these figures, the following observations are obtained:

(1) Under the design load, a certain degree of damage occurs in only a small area around the junction of steel liner and concrete while a slight damage is found in the concrete of the spiral case nasal tip. The surrounding concrete of the machine pier is undamaged. The stress level of the inlet section is slightly low and does not reach the degree of damage.

(2) Under 1.5 times water load, the damaged area increases gradually. At the same time, the area gradually appears at the lateral section of the waist at 45° and extends to the flow direction. However, the damage value is far from one. A slight damage also occurs at the top of the inlet section of the straight pipe and stator foundation at 90° . The damage phenomenon gradually expands with the increase in water load.

(3) When the water load increases 2 times, the damage between the surrounding concrete of the stator foundation and platform of the generator layer is aggravated by stress concentration. The damage value in this region reaches more than 0.9, which indicates that this region is nearly completely destroyed. The damage in concrete at the base of the 90° stator extends rapidly and expands. However, the damage value is still small.

(4) Under 2.5 times water load, the damage phenomenon in concrete is serious. At the top and waist parts of the inlet section, a high damage value appears. At the same time, damage appears at the top and waist parts of the terminal of the inlet section. Although damage occurs on these parts, the damage value of the waist in approximately 45° is small and only roughly 0.2. However, at the junction of the peripheral stator foundation and platform of the generator layer, the concrete is completely destroyed. Around a circle in

Fig. 1 Three-dimensional finite element model. **a** Model of spiral case **b** steel liner, stay ring, and guide vanes **c** stay ring and guide vanes **d** cushion

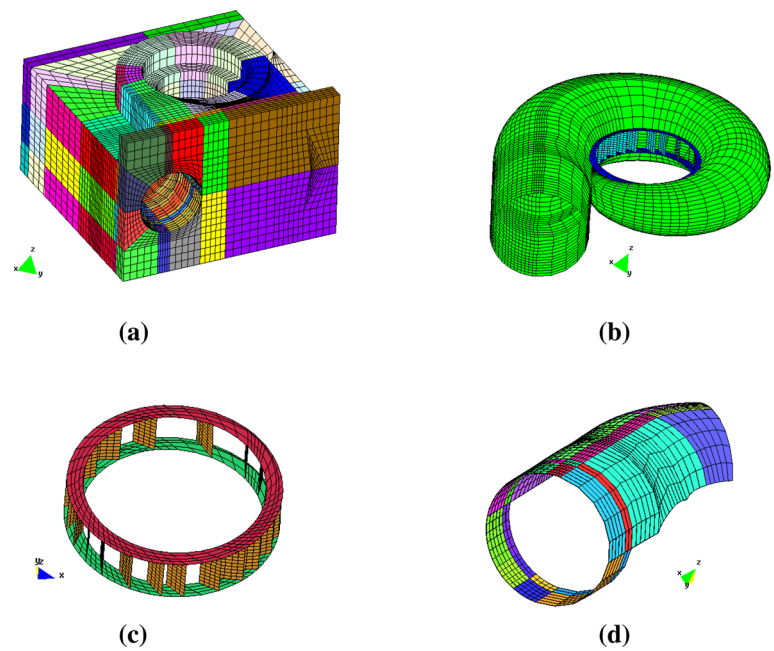


Table 1 Material parameters

| Material name | Material type | Volume weight (KN/m ³) | Elastic modulus (GPa) | Poisson ratio |
|---------------|-------------------|------------------------------------|-----------------------|---------------|
| Concrete | C25 | 24 | 28 | 0.167 |
| Steel liner | B610CF | 78 | 210 | 0.35 |
| Stay ring | S355J2G3-Z35 | 78 | 210 | 0.35 |
| Guide vanes | S355JQN | 78 | 210 | 0.35 |
| Reinforcement | II, III level | 78 | 210 | 0.35 |
| Cushion | EPS foaming sheet | 1.75 | 0.002 | 0.30 |

the plane, damage develops upstream. Furthermore, damage occurs downward near 180°, thereby forming an area with a high damage value.

(5) Under 3 times water load, the damage phenomenon in concrete is highly serious. At the top and waist parts of the inlet section, a high damage value occurs. The damage value at the waist in approximately 45° degrees is minimal, but it reaches roughly 0.5. At the junction of the peripheral stator foundation and platform of the generator layer, the concrete is completely destroyed. Damage develops upstream beside a circle in the plane. Furthermore, damage occurs downward near 180°, thereby forming an area with a large damage value.

4.2.2 Analysis of Influence of Damage on Natural Vibration Characteristics

On the basis of the analysis of concrete damage, we analyze the influence of damage on natural vibration characteristics. Table 2 shows the first ten natural frequencies of various schemes. Figure 7 indicates the decreased percentage of the

natural frequencies under various schemes. Figure 8 shows the first ten mode shapes of schemes 1, 2, and 4.

Comparing and analyzing the results of these schemes show the following observations:

(1) The action of the internal water results in damage in concrete of the spiral case structure. Unlike undamaged structure, the stiffness of damaged structure decreases, and each mode of the natural frequency declines. Under the designed load and after considering damage (scheme 2), the fundamental frequency decreases by 0.06 Hz compared with that in scheme 1 without considering damage, whereas the percentage of the first ten natural frequencies decreases by 0–1%. After considering the overload damage (schemes 3–6), the fundamental frequency decreases by 0.48, 1.94, 4.71, and 8.25 Hz, while the rates of the first ten natural frequencies decreases by 1–6, 7–20, 7–35, and 39–49%, respectively.

(2) When the internal water pressure is large, the damage in concrete is significant. The stiffness of structure decreases further, and the decreased magnitude of the natural frequencies of the spiral case structure is large. Under the designed load and after considering damage (scheme 2), the decreased

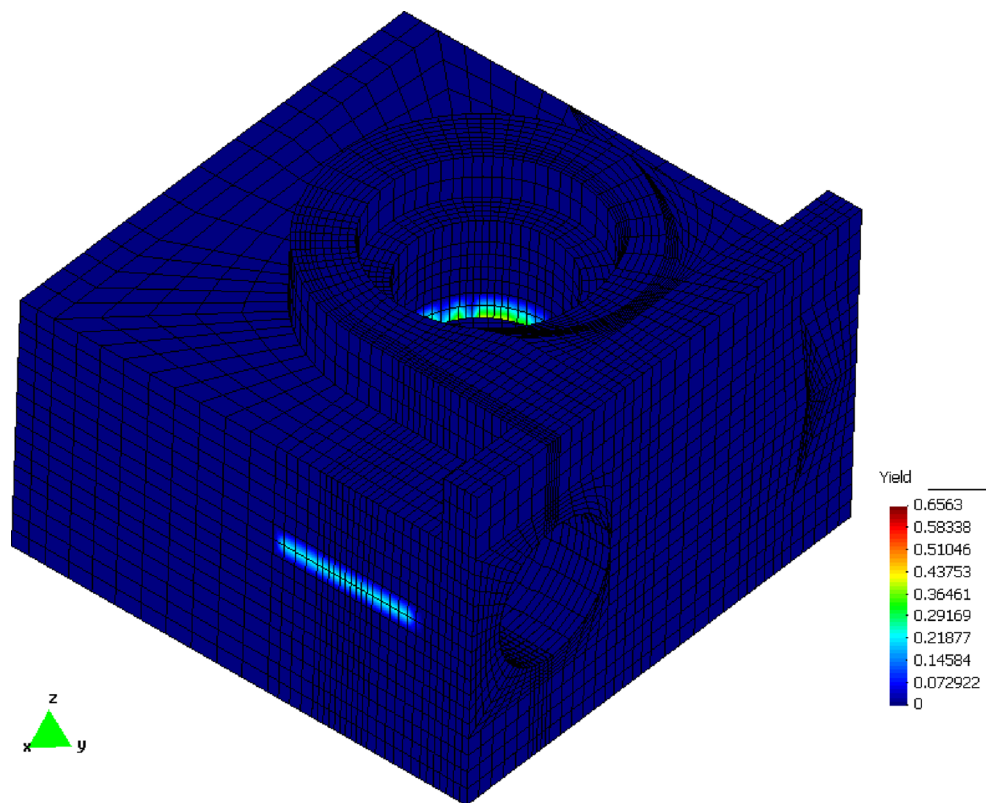


Fig. 2 Concrete damage condition of machine pier under the design load

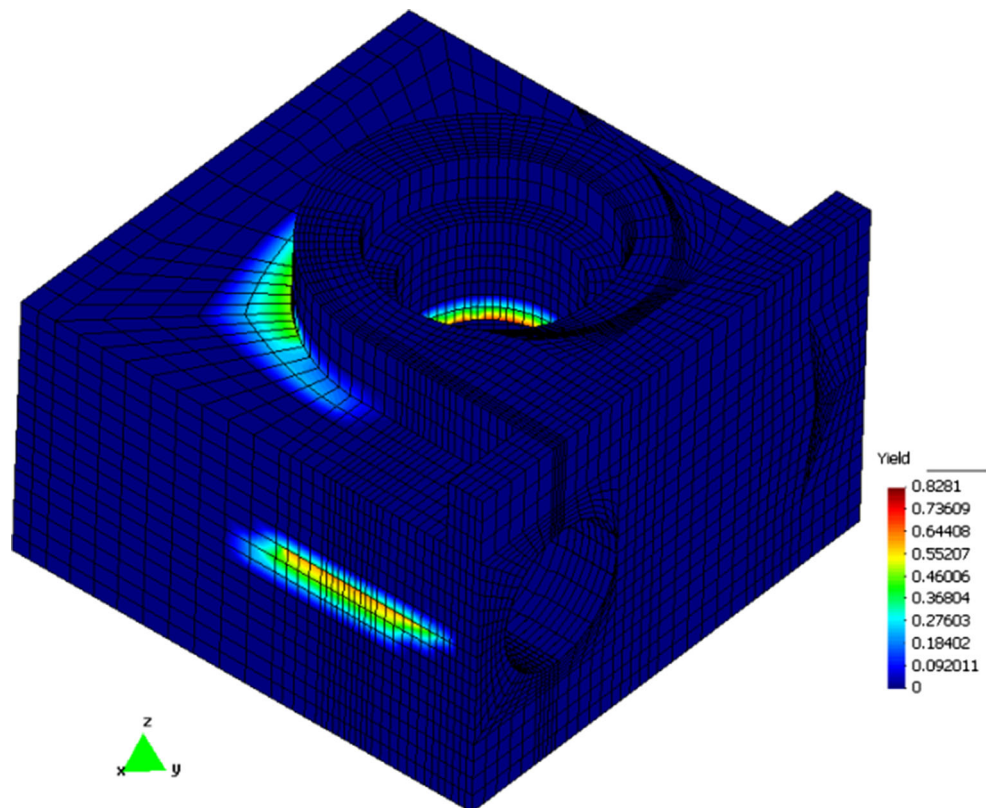


Fig. 3 Concrete damage condition of machine pier under 1.5 times water load

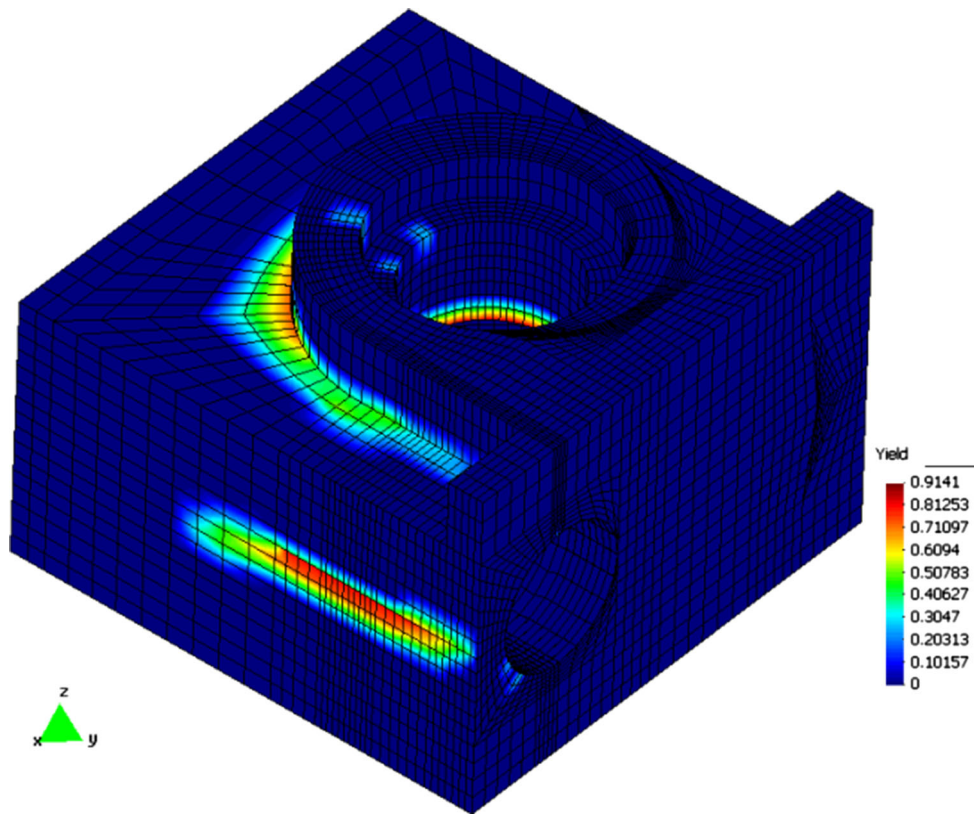


Fig. 4 Concrete damage condition of machine pier under 2 times water load

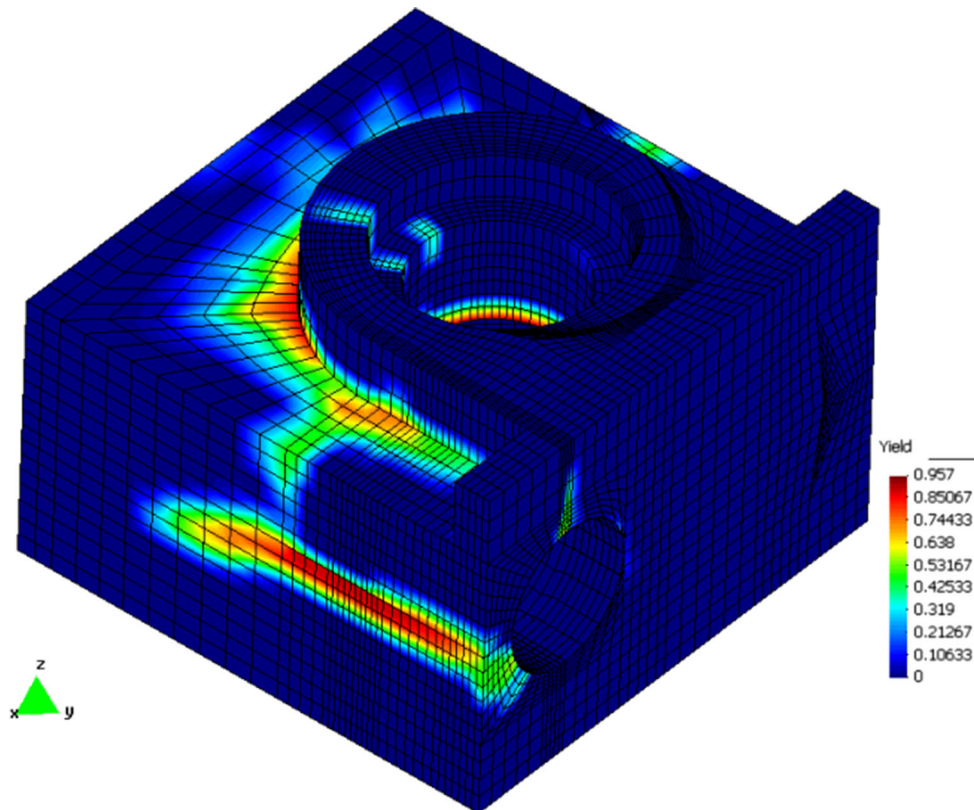


Fig. 5 Concrete damage condition of machine pier under 2.5 times water load

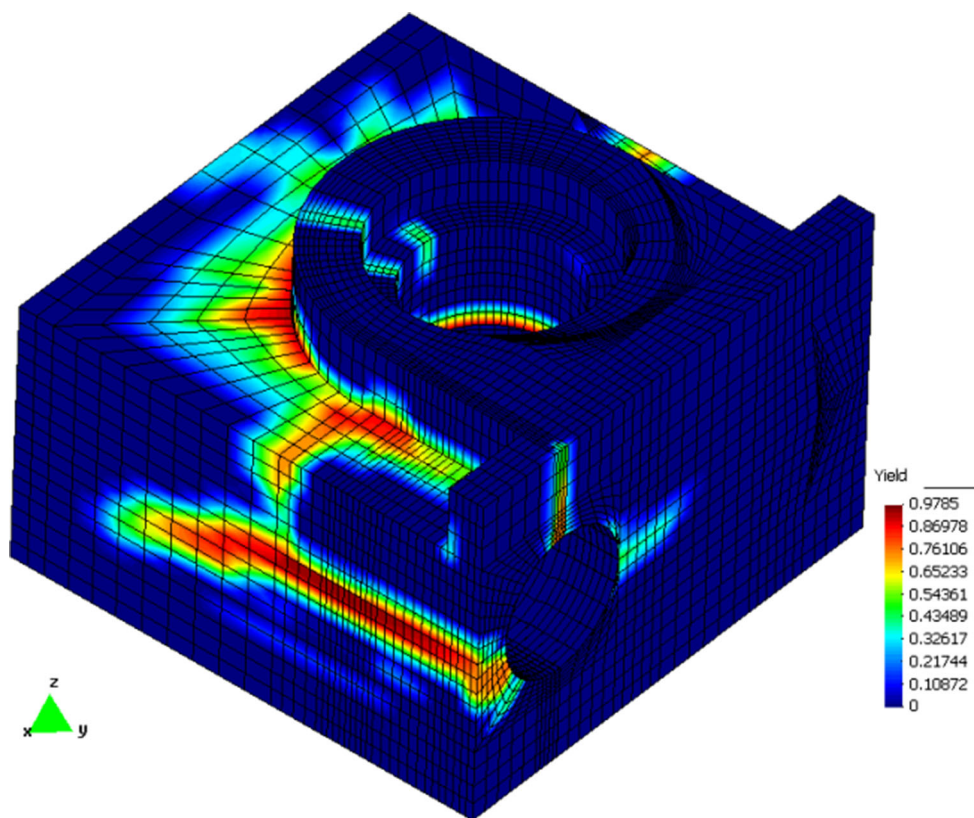


Fig. 6 Concrete damage condition of machine pier under 3 times water load

Table 2 The first ten natural frequencies of machine pier under different schemes (Hz)

| Mode | Scheme 1 | Scheme 2 | Scheme 3 | Scheme 4 | Scheme 5 | Scheme 6 |
|------|----------|----------|----------|----------|----------|----------|
| 1 | 20.76 | 20.70 | 20.28 | 18.82 | 16.05 | 12.51 |
| 2 | 21.52 | 21.47 | 21.01 | 19.46 | 16.63 | 13.04 |
| 3 | 29.04 | 29.02 | 28.65 | 27.09 | 20.95 | 16.39 |
| 4 | 32.97 | 32.84 | 31.91 | 27.40 | 24.10 | 18.52 |
| 5 | 35.60 | 35.26 | 33.76 | 30.43 | 25.46 | 19.59 |
| 6 | 36.32 | 36.24 | 35.30 | 32.15 | 27.00 | 20.66 |
| 7 | 42.97 | 42.71 | 40.50 | 34.25 | 27.75 | 22.25 |
| 8 | 44.90 | 44.71 | 43.31 | 37.99 | 30.23 | 23.02 |
| 9 | 46.64 | 46.56 | 45.64 | 41.85 | 32.01 | 23.85 |
| 10 | 49.95 | 49.69 | 48.91 | 43.92 | 34.78 | 25.84 |

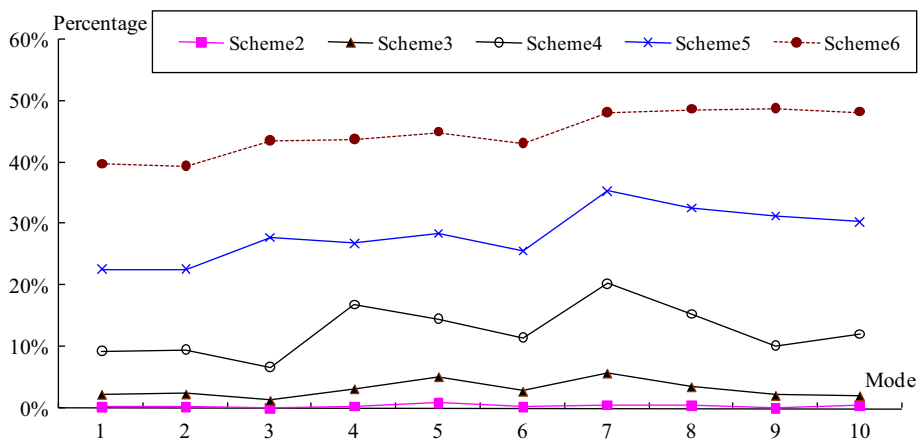
magnitude of the first ten natural frequencies is less than 1%. After considering damage under 2 times overload (scheme 4), the decreased magnitude of 8 modes is higher than 10% among the first ten natural frequencies, and the decreased magnitude of individual mode reaches 20%. However, considering damage under 3 times overload (scheme 6), the decreased magnitude of 9 modes is higher than 40% among the first ten natural frequencies. Only 1 mode is less than 40%, but it reaches 39%.

(3) Comparing the mode shapes before and after the damage in concrete shows that the mode shapes are all complex

and twisted vibrations of structure. However, after considering damage, the amplitude is generally large.

(4) Offsetting a cushion adversely affects the vibration resistance. In the six schemes, the structure mode shapes are accompanied by the vibration of the straight pipe. If other conditions occur, for example when the cushion is seriously worn after long-term operation, which disengages the steel liner and surrounding concrete, then the natural vibration characteristics of spiral case structure will significantly change. The fundamental frequency may further decrease.

Fig. 7 Comparison of the first ten natural frequencies of machine pier under various schemes



Thus, the vibration of spiral case and hydropower plant easily occurs.

4.2.3 Analysis of Influence of Damage on Resonance Safety

The vibrations of spiral case structure in a hydropower station are mainly those of the hydroelectric generating set. In addition, these vibrations are primarily caused by hydraulic, mechanical, and electromagnetic factors. Table 3 shows the forced vibration source and frequency caused by mechanical and electromagnetic forces and fluctuation in flow in accordance with the actual conditions of the Ahai Hydropower Station.

According to the regulations of the “Design Code for Hydropower House” (SL/266-2001) on the resonance check of machine pier wind cover, the ratio of the difference between natural and forced vibration frequencies should be greater than 20–30% [14]. Table 4 presents the resonance check results of the first ten natural frequencies of the spiral case structure in the Ahai Hydropower Station.

(1) In accordance with the rated speed $n_H = 88.2$ r/min and runaway speed $n_p = 170$ r/min of the Ahai Hydropower Station Unit, we can determine that the natural frequencies of the unit are 1.47 and 2.83 Hz, respectively. The natural frequencies moderately differ from the fundamental frequencies calculated under various schemes. Thus, resonance will not occur and the Ahai Hydropower Station can meet the requirements.

(2) Under the designed load with and without considering the damage in concrete, the results of resonance check are similar to each other. The difference between the natural frequencies in the range of 29–37 Hz and the vibration frequency (30.87 Hz) caused by uneven flow of guide vanes is within 30%. The difference between the natural frequencies in the range of 42–50 Hz and the vibration frequency (50 Hz) caused by a non-tight joint of the iron core base of the generator stator is within 30%. Therefore, resonance may occur. Other natural vibration frequencies of the spiral

case structure and the source may cause resonance with sufficient stagger; otherwise, resonance will not occur. Therefore, after considering the damage in concrete under the designed load, the fundamental frequency of structure insignificantly declines. However, the possible resonance range is the same as that of the case without damage, and no new possible resonance source appears.

(3) Considering the damage in concrete under 2 times overload, the difference between the natural frequencies in the range of 27–38 Hz and the vibration frequency (30.87 Hz) caused by uneven flow of guide vanes is within 30%. The difference between the natural frequencies in the range of 41–44 Hz and the vibration frequency (50 Hz) caused by the non-tight joint of the iron core base of the generator stator is within 30%. Therefore, resonance may occur. Considering the damage in concrete under 3 times overload, the difference between natural frequencies in the range of 22–26 Hz and the vibration frequency (30.87 Hz) caused by uneven flow of guide vanes is within 30%, and resonance may occur. Other natural frequencies of the spiral case structure and the source may cause resonance with sufficient stagger; otherwise, resonance will not occur. Therefore, the possible resonance range will undergo changes after considering the damage in concrete under various schemes of overload. However, no new possible resonance source exists.

5 Conclusion

In this study, the damage in concrete of large semi-cushion spiral case structure under various overload schemes, as well as the influence of different degrees of damage on the natural vibration characteristics and resonance safety of large semi-cushion spiral case structure, is investigated. The effect of damage on natural frequencies, mode shapes, and resonance safety of spiral case structure is consistent with that of the arch dam model in [5–7], powerhouse in [12], and steel frame structure in [4], respectively. The results validate the effect

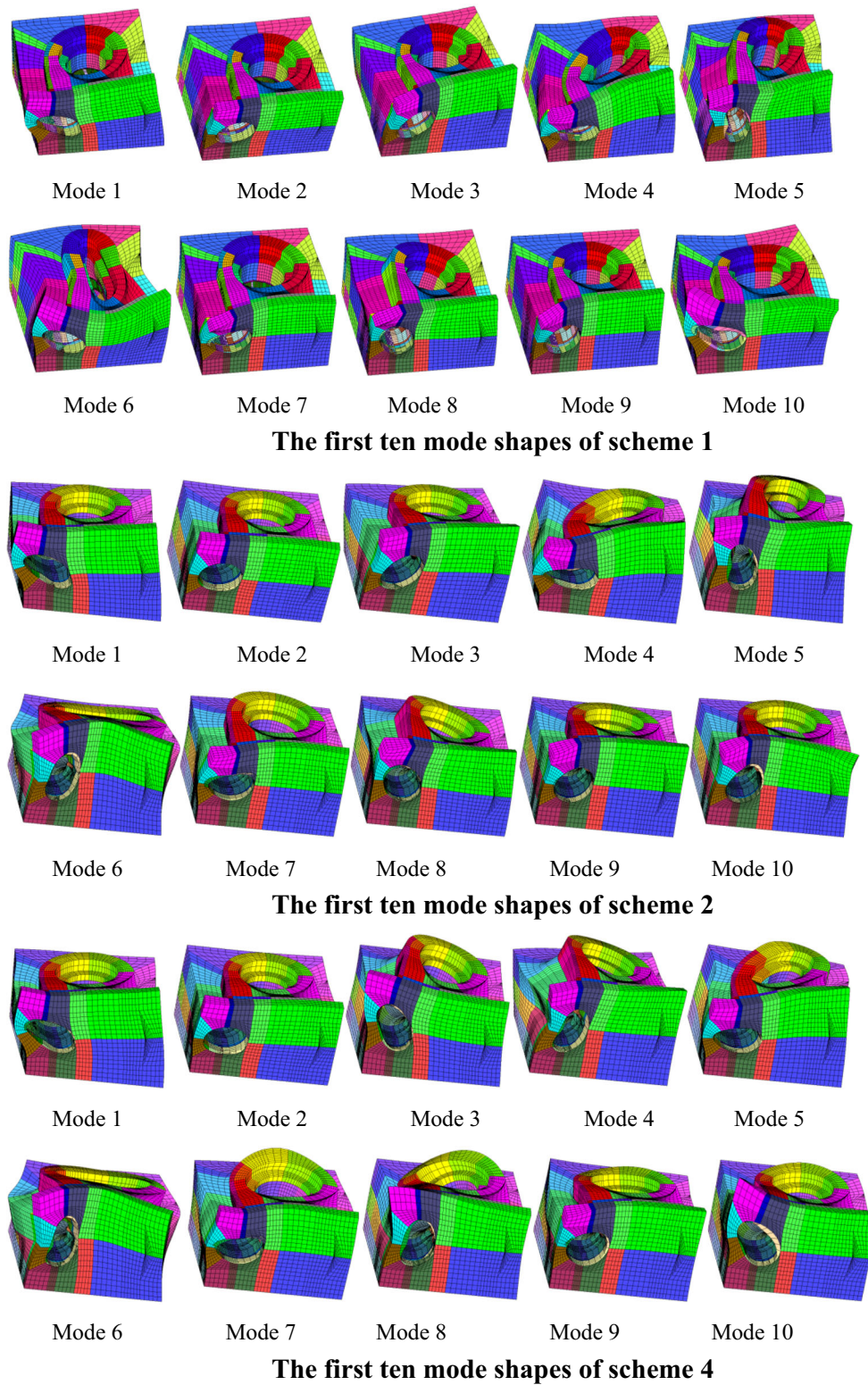


Fig. 8 The first ten mode shapes of the machine pier structure under various schemes

Table 3 Frequency of vibration source of Ahai Hydropower Station

| Type | No. | Cause of vibration | Vibration frequency (Hz) |
|--|-----|--|--------------------------|
| Vibration caused by mechanical factors | 1 | Vibration caused by eccentricity of the unit rotating part | 1.47, 2.83 |
| | 2 | Vibration caused by the collision between rotational part and fixed part | 1.47, 2.83 |
| | 3 | Vibration caused by excessive bearing clearance or superfine spindle | 1.47, 2.83 |
| | 4 | Spindle flange, thrust bearing, spindle bending | 1.47 |
| Vibration caused by hydraulic factors | 5 | Pressure fluctuation caused by cavitation of hydroturbine blade | 100, 200, 300 |
| | 6 | Runner blade-hydraulic shock pulse of guide vane | 123.48 |
| | 7 | Vibration caused by uneven flow on the guide vane | 30.87 |
| Vibration caused by electrical factors | 8 | Vibration caused by unbalanced magnetic pull | 1.47, 2.94, 4.41, 5.88 |
| | 9 | Pole frequency rotation of stator | 199.9 |
| | 10 | Vibration caused by the asymmetry of air gap of generator stator and rotor | 1.47, 2.94 |
| | 11 | Vibration caused by coil short circuit of generator | 1.47 |
| | 12 | Vibration caused by non-tight joint of iron core base of generator stator | 50, 75, 100 |

Table 4 Resonance check table for spiral case structure

| Frequency of vibration source f_{0i} (Hz) | $ (f_i - f_{0i}) / f_{0i} \times 100\%$ | | | | | | | | | | |
|---|--|-------|-------|-------|-------|-------|-------|-------|-------|-------|-------|
| | Natural vibration frequency of each mode f_i | | | | | | | | | | |
| | 1 | 2 | 3 | 4 | 5 | 6 | 7 | 8 | 9 | 10 | |
| Scheme1 | | 20.76 | 21.52 | 29.04 | 32.97 | 35.6 | 36.32 | 42.97 | 44.9 | 46.64 | 49.95 |
| | 30.87 | | | 5.93 | 6.80 | 15.32 | 17.65 | | | | |
| | 50 | | | | | | 27.36 | 14.06 | 10.2 | 6.72 | 0.1 |
| Scheme2 | | 20.70 | 21.47 | 29.02 | 32.84 | 35.26 | 36.24 | 42.71 | 44.71 | 46.56 | 49.69 |
| | 30.87 | | | 5.99 | 6.38 | 14.22 | 17.40 | | | | |
| | 50 | | | | | | 27.52 | 14.58 | 10.58 | 6.88 | 0.62 |
| Scheme4 | | 18.82 | 19.46 | 27.09 | 27.4 | 30.43 | 32.15 | 34.25 | 37.99 | 41.85 | 43.92 |
| | 30.87 | | | 12.24 | 11.24 | 1.43 | 4.15 | 10.95 | 23.06 | | |
| | 50 | | | | | | | | 24.02 | 16.30 | 12.16 |
| Scheme6 | | 12.51 | 13.04 | 16.39 | 18.52 | 19.59 | 20.66 | 22.25 | 23.02 | 23.85 | 25.84 |
| | 30.87 | | | | | | | 27.92 | 25.43 | 22.74 | 16.29 |
| | 50 | | | | | | | | | | |

1 The frequency of vibration source f_{0i} in the table is in order from low to high. 2 The blank space in the table is a non-resonance area

of damage on the dynamic characteristics of structures. From the results, the following conclusions are obtained.

(1) After the damage in concrete, the stiffness of spiral case structure decreases, while the natural frequency of each mode declines. When the damage in concrete is significant, the magnitude of the natural frequency of spiral case structure is further reduced.

(2) Before and after the damage in concrete, the mode shapes of spiral case structure are complex and twisted. However, the amplitude of the case which considers damage is generally large. The mode shapes are the main vibrations of the weak position of structure, such as those of the straight pipe section with cushion.

(3) Before and after the damage in concrete, the fundamental and natural frequencies under the rated speed of spiral case structure differ, and resonance will not occur. Thus, the spiral case structure of the Ahai Hydropower Station can meet the requirements. After considering the damage in concrete under various schemes, no new possible resonance source appears. Resonance checking shows that some degree of damage in concrete will not fatally harm the spiral case structure of the Ahai Hydropower Station.

(4) The dynamic characteristics of spiral case structure are related to its damage. Therefore, they can be used in the safety evaluation and damage identification of the spiral case structure. From the perspective of resonance safety, the spiral case structures allow for a certain degree of damage.

Acknowledgements This research work was supported by CRSRI Open Research Program (Grant No. CKWV2016386/KY), National Natural Science Foundation of China (Grant No. 51409227), and Jiangsu Planned Projects for Postdoctoral Research Funds (Grant No. 1501115B).

Compliance with ethical standards

Conflict of interest The authors declare that there is no conflict of interests regarding the publication of this paper.

References

- Dai, H.C.; Peng, P.: Selection and verification of the structural pattern of the penstock and spiral case of the TGP power-station. *Eng. Sci.* **2**, 005 (2004)
- Ditommaso, R.; Vona, M.; Gallipoli, M.R.; et al.: Evaluation and considerations about fundamental periods of damaged reinforced concrete buildings. *Nat. Hazards Earth Syst. Sci.* **13**, 1903–1912 (2013)
- Hamad, W.I.; Owen, J.S.; Hussein, M.F.M.: Modelling the degradation of vibration characteristics of reinforced concrete beams due to flexural damage. *Struct. Control Health Monit.* **22**, 939–967 (2015)
- Wang, S.S.; Ren, Q.W.: Relationship between local damage and structural dynamic behavior. *Sci. China Technol. Sci.* **55**, 3257–3262 (2012)
- Sevim, B.; Altunışık, A.C.; Bayraktar, A.: Experimental evaluation of crack effects on the dynamic characteristics of a prototype arch dam using ambient vibration tests. *Comput. Concr.* **10**, 277–294 (2012)
- Altunışık, A.C.; Günaydin, M.; Sevim, B.; et al.: CFRP composite retrofitting effect on the dynamic characteristics of arch dams. *Soil Dyn. Earthq. Eng.* **74**, 1–9 (2015)
- Altunışık, A.C.; Günaydin, M.; Sevim, B.; et al.: Retrofitting effect on the dynamic properties of model arch dam with and without reservoir water using ambient vibration test methods. *J. Struct. Eng.* **142**, 04016069 (2016)
- Altunışık, A.C.; Günaydin, M.; Sevim, B.; et al.: Dynamic characteristics of an arch dam model before/after strengthening considering reservoir water. *J. Perform. Constr. Facil.* **30**, 06016001 (2016)
- Altunışık, A.C.; Okur, F.Y.; Kahya, V.: Modal parameter identification and vibration based damage detection of a multiple cracked cantilever beam. *Eng. Fail. Anal.* **79**, 154–170 (2017)
- Altunışık, A.C.: Experimental identification of box girder bridge model under undamaged and damaged conditions considering time effect. *Comput. Concr.* **18**, 827–852 (2016)
- Zhang, C.H.; Zhang, Y.L.: Nonlinear dynamic analysis of the Three Gorge Project powerhouse excited by pressure fluctuation. *J. Zhejiang Univ. Sci. A* **10**, 1231–1240 (2009)
- Tian, Z.Q.; Zhang, Y.L.; Ma, Z.Y.; et al.: Effect of concrete cracks on dynamic characteristics of powerhouse for giant-scale hydrostation. *Trans. Tianjin Univ.* **14**, 307–312 (2008)
- Wei, W.; Li, T.C.: A new four-parameter equivalent strain for isotropic damage model. *Eng. Mech.* **22**, 92–96 (2005)
- SL 266-2001: 2001. The Ministry of Water Resources of the People's Republic of China, Design code for hydropower house